

DETC2009-86409

COMPUTED TORQUE CONTROL METHOD FOR UNDER-ACTUATED MANIPULATOR

Ambrus Zelei*

Department of Applied Mechanics
Budapest University of Technology and Economics,
Budapest, Hungary

László L. Kovács

Research Group on Dynamics of Machines and Vehicles,
Hungarian Academy of Sciences, Budapest, Hungary

Gábor Stépán

Department of Applied Mechanics
Budapest University of Technology and Economics,
Budapest, Hungary

ABSTRACT

The paper presents the dynamic analysis of a crane-like manipulator system equipped with complementary cables and ducted fan actuators. The investigated under-actuated mechanical system is described by a system of differential-algebraic equations. The position/orientation control problem is investigated with respect to the trajectory generation and the fine positioning of the payload. The closed form results include the desired actuator forces as well as the nominal load angle corresponding to the desired motion of the payload. Considering a PD controller, numerical simulation results and also experiments demonstrate the applicability of the concept of using complementary actuators for controlling the swinging motion of the payload.

1 INTRODUCTION

Cranes are widely used in industry to transport a suspended load to the place of interest. However, precise payload positioning by an overhead crane is a difficult task, since the payload exhibits pendulum-like swinging motion. Beside performance limitations, the swinging motion of the payload may result in safety concerns like damage of payload and personnel.

Many researchers have worked on the issue of anti-swing control of overhead crane systems ([1], [2], [3], [4]). The goal of the different control algorithms is to achieve both position regulation and anti-swing control. This means that the payload should move along a prescribed trajectory in such a way that the load angle oscillation is suppressed as quickly as possible. Other crane designs may compensate for the swinging of the load by using more than one supporting cables. For example, the NIST RoboCrane [5] utilizes a cable based inverted Stewart platform in order to provide improved load stability. Obviously, using a parallel mechanism enables also the 6

degrees of freedom payload control; however, the workspace of this robotic crane is limited by the cable supports.

A novel field of using crane-like systems is service robotics, where sharing the place with humans is an important problem. Reference [6] presents a ceiling based mobile robot platform, where the cart of the overhead crane system is substituted by a magnetic support/transport system and, instead of cables, the payload is attached to a platform that is oriented by 3 telescopic actuators. Evidently, this concept solves the problem of swinging payloads, while also provides space division between the robot and obstacles without the ultimate need of time-sharing and -scheduling. On the other hand, while the control problem is simpler in this case, the mechanical structure of this device is much more complex than that of an overhead crane. In addition, the vertical workspace of such a robot is limited.

Taken into account the above considerations, one can conclude that using simple complementary actuators may be advantageous when relatively small payloads are to be transported and there is also a need for fine positioning and orienting the carried load.

This paper investigates the concept of using complementary cable-winding motors and ducted fans for payload control. Since partially the ducted fans accelerate the payload the weight of the payload should not be large compared to the maximal thrust force. Together with these additional actuators, the payload becomes a kind of 'swinging actuator'. Figure 1 shows the design of the prototype of this under-actuated manipulator. In the case we consider here, three cables orientate the swinging load, while two parallel-direction ducted fans are used for stabilizing the motion of the payload along the desired trajectory. The thrust provided by the ducted fans makes it also possible to move the payload even if the

* Author of correspondence, Phone: +36 1 463 1369, Fax: +36 1 463 3471, Email: zelei@mm.bme.hu.

cable suspension point does not move at all. Nevertheless the suspension point is moved during normal operation of the system. Further equipments can be connected to the platform via a special mechanical connection interface.

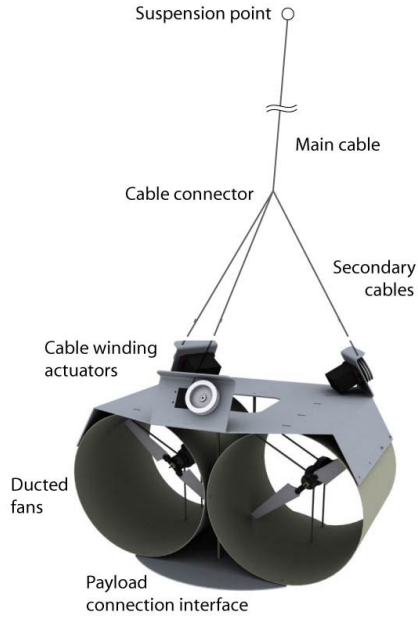


Figure 1. Concept of the swinging actuator

2 PLANAR MODEL OF THE ACTUATOR

In this study, we investigate the reduced planar case of the swinging actuator. The mechanical model of the investigated planar crane-like manipulator system is presented in Figure 2. Only two cables orientate and one ducted fan stabilizes the swinging load. In this model, the suspension point O is considered to be fixed in a certain position. The bar AB models the body of the swinging actuator itself, and also the payload with total weight m and mass moment of inertia J_C . The centre of gravity affected also by the attached payload is denoted by point C . The main suspending cable between point O and D has a constant length L , while the secondary cables AD and BD are considered to be wound by DC motors fixed on the swinging actuator at A and B . In addition, the force F_T denotes the thrust of the ducted fan parallel to the bar and placed below the system.

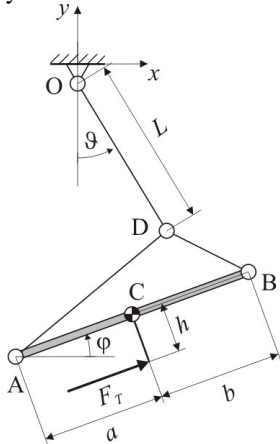


Figure 2. Planar model of the swinging actuator

According to Figure 2, the system has 4 degrees of freedom, which can uniquely be described by the load angle ϑ of the main suspending cable, the tilt angle φ of the swinging platform and the coordinates x and y of the centre of gravity C . The number of the generalized coordinates is $\dim_q = 4$. The task is described by the position coordinates of C and the tilt angle φ thus the dimension of the task is $\dim_t = 3$. Since the task requires less than the available degrees of freedom, the swinging actuator is kinematically redundant. However, the system can only be actuated by 3 control inputs so it is also under-actuated. One actuator is the thrust force F_T of the ducted fan, while the torques of the cable winding motors provide the cable forces F_A and F_B acting at the points A and B respectively (see Figure 2). The number of the control inputs is $\dim_u = 3$.

In case of most of the (under-)actuated manipulators, the dimension of the available control inputs is higher than the dimension of the task. Thus, the following inequality holds:

$$\dim_u \geq \dim_t. \quad (1)$$

In the $\dim_u = \dim_t$ case, the kinematic redundancy is automatically dissolved with the help of the $(\dim_q - \dim_u)$ number of differential equations beside of the \dim_t number of algebraic equations of task definition and the generalized coordinates can be calculated uniquely with respect to the task. The investigated manipulator belongs to this class with $\dim_q = 4$, $\dim_u = \dim_t = 3$.

Note that in the $\dim_u > \dim_t$ cases, the system is kinematically redundant, which means that the generalized coordinates can not be determined uniquely with respect to the task, and the standard optimization algorithms can be applied (see:[8], [9], [10]).

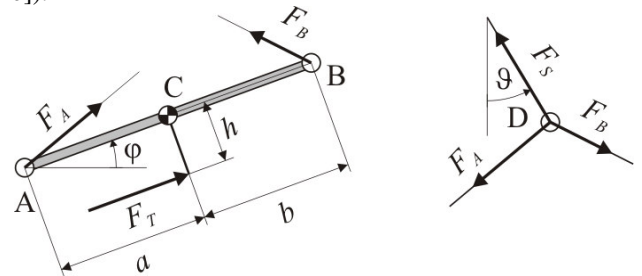


Figure 3. Free body diagrams of the actuator

In order to derive the equations of motion, the following set of redundant coordinates is introduced

$$\mathbf{x} = [\varphi \ x \ y \ x_D \ y_D]^T, \quad (2)$$

where (x, y) , and (x_D, y_D) are the Cartesian coordinates of the centre of gravity C and the cable connection point D of the three cables, respectively. Although four coordinates are needed only, it is easier to derive the cable force as the function of the redundant coordinates (2), in this case. Then the three active forces and the ideal constraining force F_S of the suspension are as follows

$$\begin{aligned} \mathbf{F}_A &= \lambda_A (\mathbf{r}_D - \mathbf{r}_A), \\ \mathbf{F}_B &= \lambda_B (\mathbf{r}_D - \mathbf{r}_B), \\ \mathbf{F}_T &= F_T [\cos \varphi \ \sin \varphi]^T, \\ \mathbf{F}_S &= -\lambda \mathbf{r}_D, \end{aligned} \quad (3)$$

where λ is the Lagrangian multiplier related to the suspension force. The cable control forces \mathbf{F}_A and \mathbf{F}_B are expressed in a similar form by using the scalar time-dependent scaling factors λ_A and λ_B , although they are not constraining forces, rather virtual stiffnesses that are controlled actively by means of the winders at A and B. The position vectors can clearly be expressed by the geometry of the structure given by the parameters a, b, h and L (see in Figure 3).

The redundant set of coordinates defined in (2) and constraining and control forces in (3) lead to the following Lagrangian equations of the first kind in the form

$$J_C \dot{\varphi} + (a\lambda_A - b\lambda_B)(x - x_D) \sin \varphi - (a\lambda_A - b\lambda_B)(y - y_D) \cos \varphi - F_T h = 0, \quad (4)$$

$$m\ddot{x} + (\lambda_A + \lambda_B)(x - x_D) - (F_T + a\lambda_A - b\lambda_B) \cos \varphi = 0, \quad (5)$$

$$m\ddot{y} + (\lambda_A + \lambda_B)(y - y_D) - (F_T + a\lambda_A - b\lambda_B) \sin \varphi + mg = 0, \quad (6)$$

$$(a\lambda_A - b\lambda_B) \cos \varphi + (\lambda_A + \lambda_B + \lambda) x_D - (\lambda_A + \lambda_B) x = 0, \quad (7)$$

$$(a\lambda_A - b\lambda_B) \sin \varphi + (\lambda_A + \lambda_B + \lambda) y_D - (\lambda_A + \lambda_B) y = 0, \quad (8)$$

together with the single geometric constraint equation

$$x_D^2 + y_D^2 - l^2 = 0. \quad (9)$$

The set of equations of motions (4-9) consists of three differential equations and three algebraic ones. Due to the appropriate selection of the redundant coordinates, one can recognize that the algebraic equations (7-9) can be solved for x_D, y_D and λ in closed form

$$x_D = \frac{\lambda_A(x - a \cos \varphi) + \lambda_B(y + b \cos \varphi)}{\lambda_A + \lambda_B + \lambda}, \quad (10)$$

$$y_D = -\sqrt{L^2 - x_D^2}, \quad (11)$$

$$\lambda = \frac{1}{2} \left(-C_2 + \sqrt{C_2^2 - 4C_1} \right), \quad (12)$$

with

$$C_1 = (\lambda_A + \lambda_B)^2 - \frac{((a\lambda_A - b\lambda_B) \cos \varphi - (\lambda_A + \lambda_B)x)^2}{L^2} + \frac{((a\lambda_A - b\lambda_B) \sin \varphi - (\lambda_A + \lambda_B)y)^2}{L^2},$$

$$C_2 = 2(\lambda_A + \lambda_B).$$

If these formulae are substituted into the system of 3 second order differential equations (4-6), the actual motion can be integrated for given actuator force functions $\lambda_A(t), \lambda_B(t)$ and $F_T(t)$. So the differential algebraic system can be reduced to a system of ordinary differential equations.

3 COMPUTED TORQUE CONTROL

When computed torque control technique is to be applied, the actuator forces have to be calculated based on the desired trajectory of the swinging actuator given by the functions $x_d(t), y_d(t)$ and $\varphi_d(t)$. If these functions are prescribed, then using the algebraic equations (7-8) and writing the constraint equation in the form of two separate equations with the parameter ϑ :

$$x_D = L \sin \vartheta \quad y_D = -L \cos \vartheta \quad (13)$$

yield the load (nutation) angle as the function of the prescribed coordinates and accelerations as

$$\vartheta = \arctan \frac{-J_C \dot{\varphi}_d c_d + mh\ddot{x}_d - mx_d((\ddot{y}_d + g) c_d - \ddot{x}_d s_d)}{J_C \dot{\varphi}_d s_d - mh(\ddot{y}_d + g) + my_d((\ddot{y}_d + g) c_d - \ddot{x}_d s_d)}, \quad (14)$$

where $s_d = \sin \varphi_d$ and $c_d = \cos \varphi_d$ according to the standard robotic notation. Since equations (4-6) are linear in the actuator force functions $\lambda_A(t), \lambda_B(t)$ and $F_T(t)$, the substitution of the above results in

$$\mathbf{A} \mathbf{f} + \mathbf{b} = \mathbf{0} \quad (15)$$

with

$$\mathbf{A} = \begin{bmatrix} -h & a(x_d - x_D) s_d - a(y_d - y_D) c_d & -b(x_d - x_D) s_d + b(y_d - y_D) c_d \\ -c_d & x_d - x_D - a c_d & x_d - x_D + b c_d \\ -s_d & y_d - y_D - a s_d & y_d - y_D + b s_d \end{bmatrix}$$

$$\mathbf{f} = [F_T \quad \lambda_A \quad \lambda_B]^T, \quad (16)$$

$$\mathbf{b} = [J_C \dot{\varphi}_d \quad m\ddot{x}_d \quad m(g - \ddot{y}_d)]^T.$$

This makes it possible to calculate the desired actuator forces in closed form. Then the computed torque controller can be formulated as

$$\mathbf{z} = [x \quad y \quad \varphi]^T,$$

$$\mathbf{z}_d = [x_d \quad y_d \quad \varphi_d]^T,$$

$$\mathbf{f}_{err} = \mathbf{K}_P (\mathbf{z}_d - \mathbf{z}) + \mathbf{K}_D (\dot{\mathbf{z}}_d - \dot{\mathbf{z}}),$$

$$\mathbf{f}_{control} = \mathbf{f} + \mathbf{f}_{err},$$

where \mathbf{z} denotes the controllers feedback, and $\mathbf{f}_{control}$ is the control output that regulates the swinging actuator around the desired trajectory. The matrices \mathbf{K}_P and \mathbf{K}_D contain the proportional and derivative feedback gains for the state variables x, y and φ . Note, that the force functions $\lambda_A(t)$ and $\lambda_B(t)$ in \mathbf{f} do not give the actuator forces directly. According to equation (3), the calculation of the control forces (torques) of the cable winding motors requires also the feedback of the load angle. The scaling parameter functions $\lambda_A(t)$ and $\lambda_B(t)$ can be interpreted as time dependent stiffness values of the cables if they were springs. In this sense, the controller in (17) behaves similarly to active suspension systems with varying stiffness.

4 SIMULATION RESULTS

To demonstrate the applicability of the controller presented in equations (17), an example is considered when the swinging actuator should move from a steady state to another point with zero tilt angle (see Table 1). In this case, the desired trajectory can easily be given by an analytical formula. This trajectory together with the mass, the inertia and the geometry information are provided in Table 1.

Based on the parameters listed in Table 1 and Table 2, the actuator forces are calculated according to equations (13-16). The results presented in Figure 6 show the actuator forces required for the open loop control of the swinging actuator. The load angle ϑ can be seen on Figure 4.

Table 1. Mechanical and geometry data of the swinging actuator and the desired path

<i>Mechanical Parameters of the swinging actuator</i>			
Total weight	m	5 [kg]	
Moment of inertia	J_C	0.02 [kg m ²]	
Main cable length	L	0.3 [m]	
Geometric data	a	0.18 [m]	
Geometric data	b	0.22 [m]	
Geometric data	h	0.1 [m]	
<i>Desired trajectory</i>			
Position of C	$x_d(t)$	$(0.2/\pi) \arctan(4(t-5))$ [m]	
Position of C	$y_d(t)$	$-0.65 - (0.2/\pi) \arctan(4(t-5))$ [m]	
Tilt angle	$\varphi_d(t)$	0 [rad]	

Table 2. Initial conditions for calculating the nominal actuator forces and the corresponding initial deviation used in the simulation

<i>Initial value</i>		<i>Deviation</i>	
$x(0)$	0.1 [m]	$x_{err}(0)$	0.05 [m]
$y(0)$	-0.55 [m]	$y_{err}(0)$	0.05 [m]
$\varphi(0)$	0 [rad]	$\varphi_{err}(0)$	0.3 [rad]
$\dot{x}(0)$	0 [m/s]	$\dot{x}_{err}(0)$	0 [m/s]
$\dot{y}(0)$	0 [m/s]	$\dot{y}_{err}(0)$	0 [m/s]
$\dot{\varphi}(0)$	0 [rad/s]	$\dot{\varphi}_{err}(0)$	0 [rad/s]

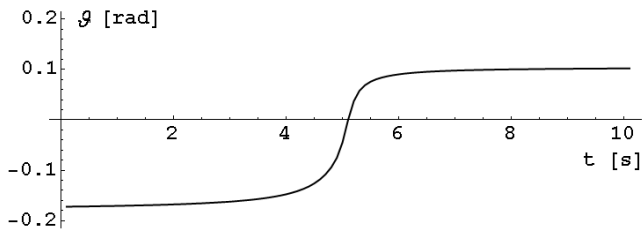


Figure 4. Load angle ϑ corresponding to the desired motion of the swinging actuator

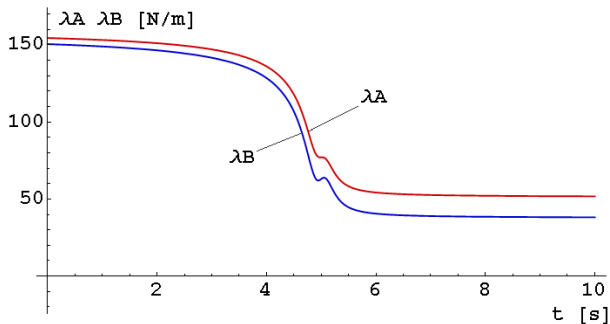


Figure 5. The calculated scaling factors $\lambda_A(t)$, $\lambda_B(t)$

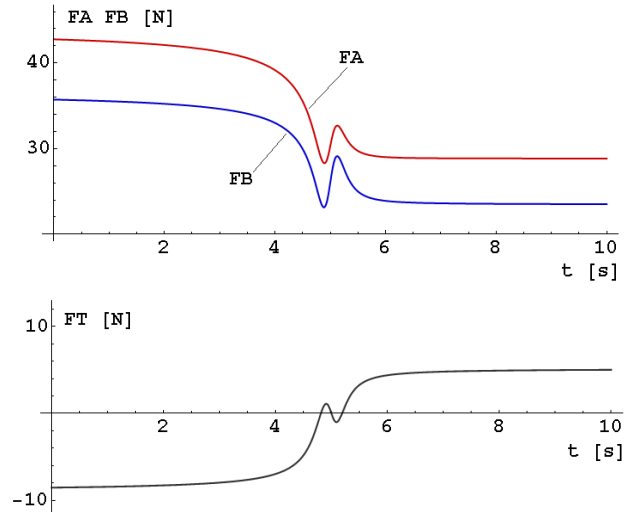


Figure 6. The nominal actuator forces F_A , F_B and F_T

For testing the controller in (17), the initial position of the swinging actuator was shifted by 50 mm deviation in both x and y directions, and the tilt angle φ was set to 0 with 0.3 rad initial error (see Table 2). The proportional and derivative gain matrices were selected in SI units as

$$K_P = \begin{bmatrix} 2 & 0 & 0 \\ 0 & 2 & -50 \\ 0 & 2 & 50 \end{bmatrix} \quad K_D = \begin{bmatrix} 80 & 0 & 0 \\ 0 & 180 & -80 \\ 0 & 180 & 80 \end{bmatrix} \quad (18)$$

The gain values were tuned via trial and error based simulations. The horizontal position error $x-x_d$ was used for calculating the necessary thrust force of the ducted fan, while the cable forces are calculated according to the vertical position error $y-y_d$ and the orientation error $\varphi-\varphi_d$.

Despite of the large initial deviation from the desired trajectory, Figure 7 shows that the controller with the selected gains (18) quickly regulates the motion of the centre of gravity and also the tilt angle. It follows exactly the prescribed linear trajectory after a few seconds only.

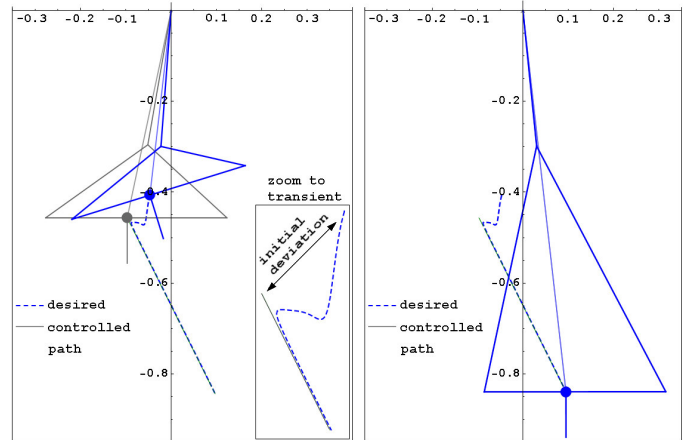


Figure 7. Controlled motion of the swinging actuator. Left: initial configuration, right: configuration at the end of the path

The time characteristics of each control variables and also that of the load angle are presented in Figure 8. Beside the regulation of the position error of the swinging actuator, the fast settling of the tilt angle can also be observed.

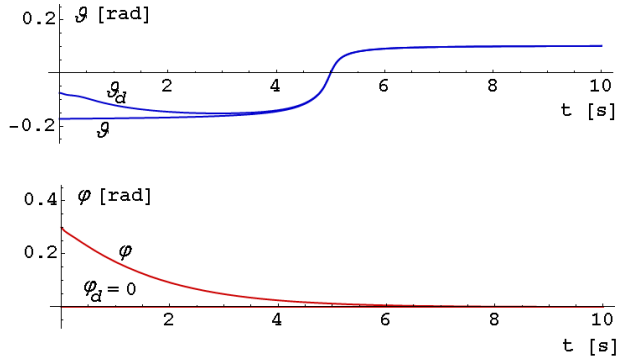


Figure 8. Comparison of the desired and realized motion during simulation: load angle and tilt angle

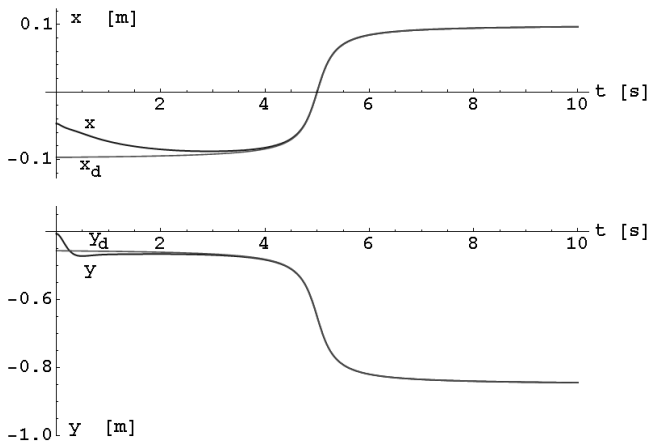


Figure 9. Comparison of the desired and realized motion during simulation: x and y positions

5 PROTOTYPE EXPERIMENT

Laboratory experiments have been carried out with the prototype of the swinging manipulator (see Figure 10). The communication and supply cables go down to the swinging actuator along the main cable. Because the above control approach was tested in space and not just in the vertical plane, small cross-direction secondary fans were also applied during the experiments.

In the spatial case, numerical methods were used instead of the analytical formulas derived for the planar model. The path was given by a high degree polynomial interpolation between the target points.

The position of the swinging actuator was measured by an ultrasonic system. Figure 11 and Figure 12 show the measured motion around the desired trajectory. The averaged error was about 15mm (10,7%) due to the continuous perturbation caused by the noisy signal of the ultrasonic measuring system, on which the PD controller was based. The accuracy of the control was also influenced by the airflow and the elasticity of the main and secondary suspending cables. These effects are neglected in the mechanical model presented in section 2.

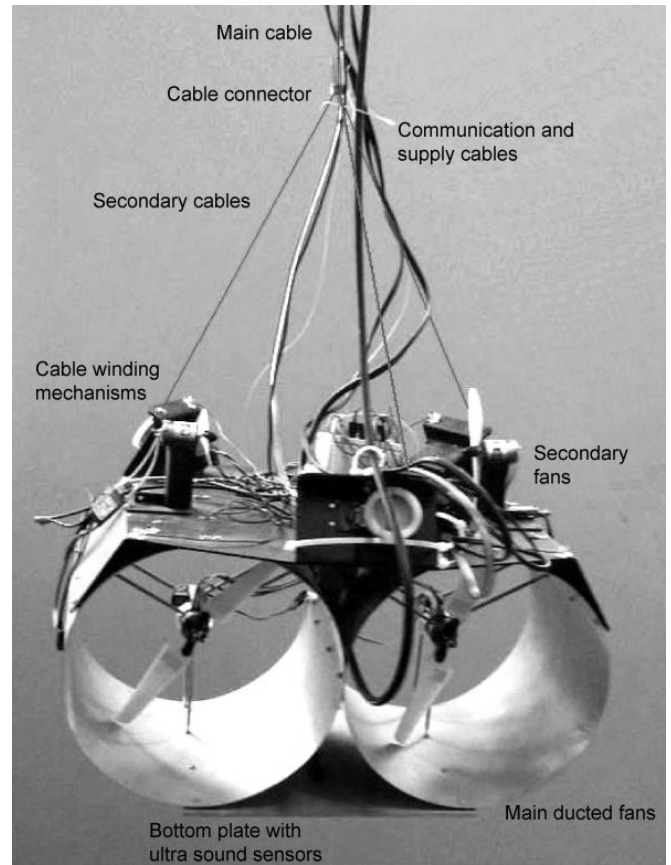


Figure 10. Prototype of the swinging actuator

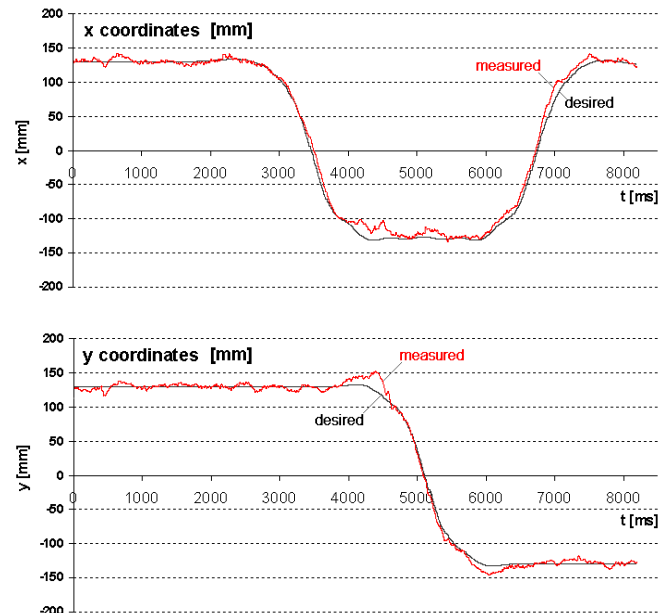


Figure 11. Time history of the desired and measured space coordinates

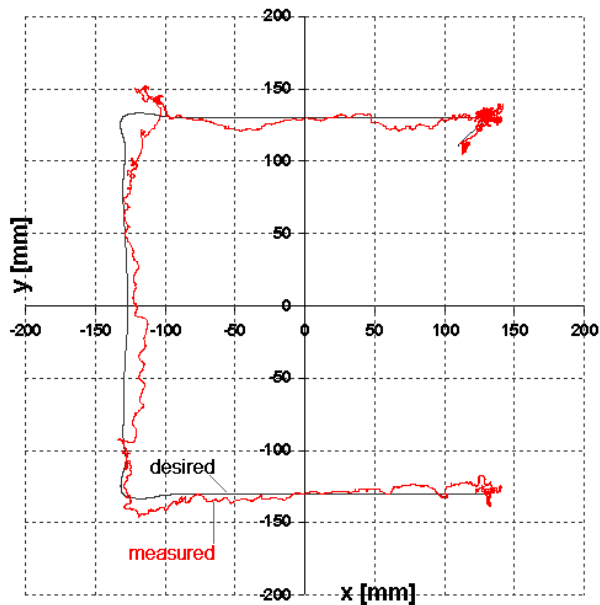


Figure 12. Desired and measured path

6 CONCLUSIONS

The dynamics of a planar crane-like structure with complementary actuators were analyzed with respect to its applicability for transporting relatively small payloads along a desired trajectory. The system is redundant and under-actuated. In the investigated planar case, it was shown that using the analytically derived formulae for computing the desired actuator forces, a simple PD controller could effectively provide the desired motion of the system using the classical computed torque control method. This way, the otherwise undesirable swinging of the manipulator can be utilized to achieve fast trajectory following.

Future work includes the systematic design of the control parameters based on detailed stability analysis and the application/extension of the concept to three dimensional swinging actuator systems. The swinging actuators will be useful in many applications far beyond the crane systems, like in case of cooperative and collaborative robots.

ACKNOWLEDGEMENTS

This work was supported in part by the Hungarian National Science Foundation under grant no. OTKA K068910, the European Union FP6 ACROBOTER project under grant no. IST-2006-045530 and the Hungarian Academy of Sciences under grant no. MTA-NSF/103.

REFERENCES

- [1] Fang Y., Dixon W. E., Dawson D. M., Zergeroglu E., 2001, "Nonlinear Coupling Control Laws for a 3-DOF Overhead Crane System", In *Proceedings of the 40th Conference on Decision and Control*, Orlando, Florida USA, December, 2001, 3766-3771.
- [2] Rodrigues F. O., Yu W., Moreno-Armendariz M. A. (2007). Anti-swing control with hierarchical fuzzy CMAC compensation for an overhead crane, In *Proceedings of the 22nd IEEE International Symposium on Intelligent Control (Part of IEEE Multi-Conference on Systems and Control)*, Singapore, 1-3 October, 2007, 333-338.
- [3] Omar H. M., Nayfeh A. H. (2003): *Control of gantry and tower cranes*. Research Report, Virginia Polytechnic Institute and State University, 2003.
- [4] Lew J. Y., Khalil A. (2000). Anti Swing Control of a Suspended Load with a Robotic Crane, In *Proceedings of the American Control Conference*, Chicago, Illinois, June 2000, 1042-1046.
- [5] Albus J.S., Bostelman R.V. and Dagalakis N.G. (1992), The NIST ROBOCRANE: A Robot Crane, *Journal of Robotic Systems*, Wiley, New York, NY (July 1992).
- [6] Sato T., Fukui R., Mofushita H. Mori T. (2004). Construction of Ceiling Adsorbed Mobile Robots Platform Utilizing Permanent Magnet Inductive Traction Method, In *Proceedings of 2004 IEEE/RSJ International Conference on Intelligent Robots and Systems*, September 28 -October 2, 2004, Sendai, Japan, 552-558.
- [7] Jalon J.G., Bayo E. (1994). *Kinematic and Dynamic Simulation of Multibody Systems: The Real-Time Challenge*, Springer-Verlag, New-York, 1994.
- [8] O. Khatib. *Commande dynamique dans l'espace opérationnel des robots manipulateurs en présence d'obstacles*. PhD thesis, Ecole Nationale Supérieure de l'Aéronautique et de l'Espace, Toulouse, 1980.
- [9] C. Klein and B. Blaho. Dexterity measures for the design and control of kinematically redundant manipulators. *Int. J. Robotics Research*, 6(2): pp 72–83, 1987.
- [10] J. M. Hollerbach and K. C. Suh. Redundancy resolution of manipulators through torque optimization. *Int. Conf. Robotics and Automation*, pp 1016–1021, St. Louis, MS, 1985.
- [11] L. Udawatta, K. Watanabe, K. Izumi, K. Kiguchi. Control of Underactuated Robot Manipulators Using Switching Computed Torque Method: GA Based Approach. *Int. J. Soft Comput.*, 8(1): pp 51-60, 2003